Anomalous Photoluminescence Stokes Shift in CdSe Nanoparticle/Carbon Nanotube Hybrids

Austin J. Akey,[†1] *Chenguang Lu,*[†1] *Lijun Wu,*[2] *Yimei Zhu,*[2] *and Irving P. Herman*[*1]

[1] Department of Applied Physics and Applied Mathematics

Columbia University

New York, NY 10027

[2] Department of Condensed Matter Physics, Brookhaven National Laboratory

Upton, NY 11973

[†] *These authors contributed equally*

[*] *Corresponding author*

Supplemental Information

1) CdSe Nanoparticle Synthesis and Hybrid Preparation

As previously reported[1], hybrids of CdSe nanoparticles and single-walled carbon nanotubes (SWNT) can be prepared by a process of capping the nanoparticles with pyridine followed by sonication in the presence of SWNT and repeated washing to remove unbound particles. CdSe nanoparticles were prepared using conventional colloidal synthesis procedures, starting with CdO as the precursor and producing nanoparticles with sizes ranging from 1.4 to 3.4 nm in radius, capped with trioctyl phosphene oxide (TOPO).

CdSe/ZnS core shell nanoparticles were formed by a modified SILAR method[2]. CdSe nanoparticles were dispersed in molten hexadecylamine and degassed at 100°C for 30 min. Then at 200°C, 1 mL 0.04 M zinc oleate in octadecene solution was injected followed by 1 mL of 0.04 M sulfur in octadecene solution 5 min later. The mixture was kept at 200°C for 30 min, and this procedure was repeated, followed by 30 min at 240°C, and then extraction and purification as

above.

2) Additional Optical Analysis Figures

Figure S1 shows the absorption spectra of NPs, (HiPCO) SWNTs, and hybrids made from these, as reproduced from Ref. 1.

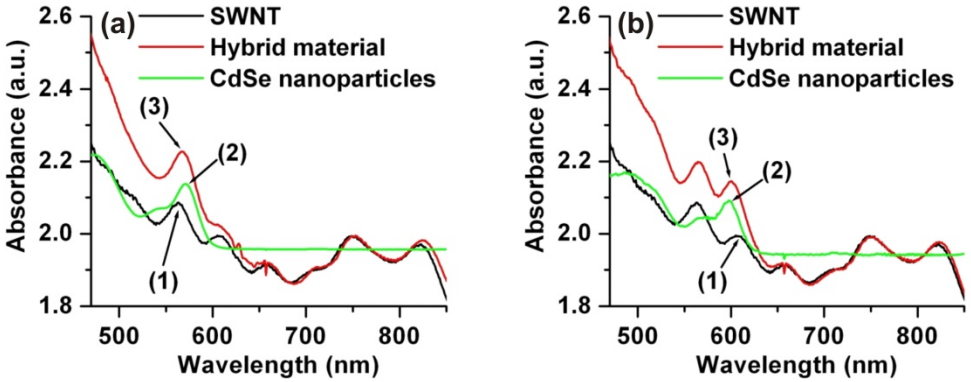

Figure S1. (a) Visible absorption of HiPCO SWNTs, 1.8 nm radius CdSe nanoparticles, and the corresponding hybrid material. Peak (1) is the SWNT transition peak at 562 nm. Peak (2) is the first exciton peak of CdSe nanoparticles at 571 nm. These peaks contribute to the absorption maximum at 568 nm [peak (3)] for the hybrid material; (b) Visible absorption of HiPCO SWNTs, 2.2 nm radius CdSe nanoparticles, and the corresponding hybrid material, with the peaks at 598 nm, 607 nm, 600 nm, respectively. The vertical scales differ for each curve. All samples are measured in pyridine. (Reproduced from Ref. 1.)

Figure S2 presents the Stokes shifts of the unbound NPs and hybrids as a function of particle radius, along with the model predictions described below. The difference of these shifts is presented in Fig. 3 in the main paper.

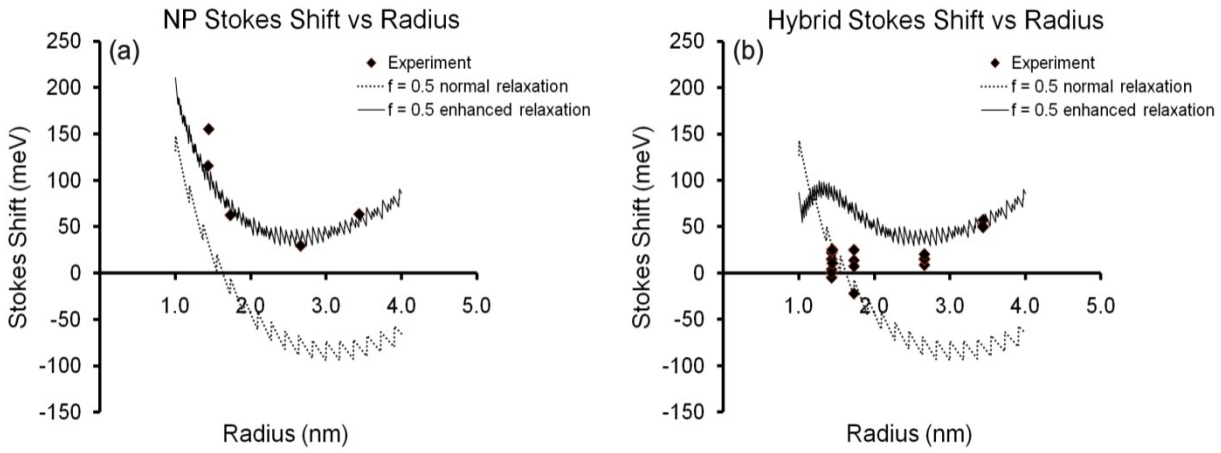

Figure S2. (a) Stokes shift of CdSe NPs versus NP radius. (b) Stokes shift of HiPCO-SWNT hybrid material versus NP radius. The solid line represents the results of the phonon model with fast energy relaxation (increased by a factor of 4 above the absorption edge); the dotted line represents model results without fast energy relaxation (i.e., with energy relaxation rate equal for all states). Here $f = 0.5$ and $\Delta = 1$ meV.

3) Transmission Electron Microscopy of Hybrids formed using Separated SWNTs

Transmission electron microscopy images (100 keV, JEOL JEM-100CX) of the hybrids made using the arc-discharge SWNTs enriched in either semiconducting or metallic tubes are shown in Fig. S3. They show similar binding of the NPs only to tubes, as seen in Fig. 1 in the main paper and in Ref. 1, for the hybrids made with unseparated HiPCO SWNTs.

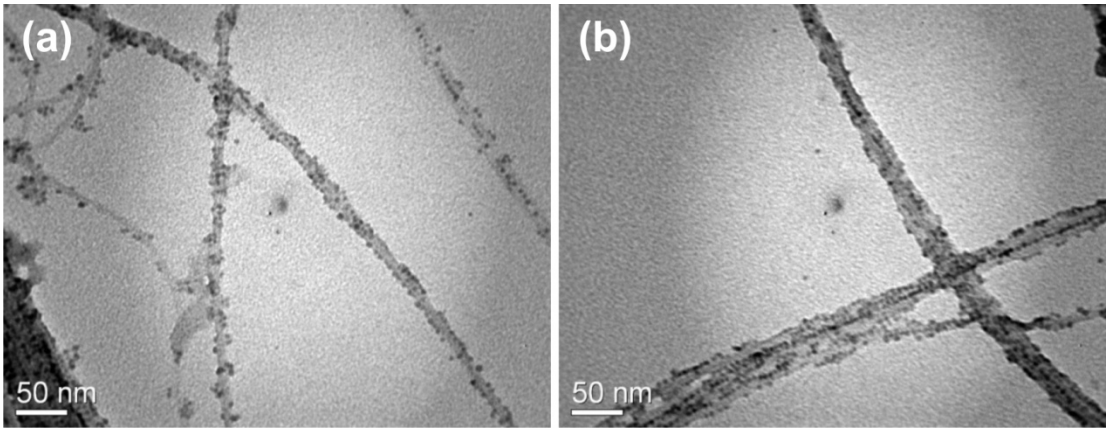

Figure S3. TEM micrographs (100 keV) of (a) hybrid of 2.0 nm radius CdSe NPs and enriched semiconducting arc-discharge SWNTs and (b) hybrid of 1.8 nm radius CdSe NPs and enriched metallic arc-discharge SWNTs. Nanoparticles are seen to decorate both materials with similar density and without measurable size-selective attachment.

4) Additional Photoluminescence Model Figures

The results of several model simulations are given in Figs. S4 –S7.

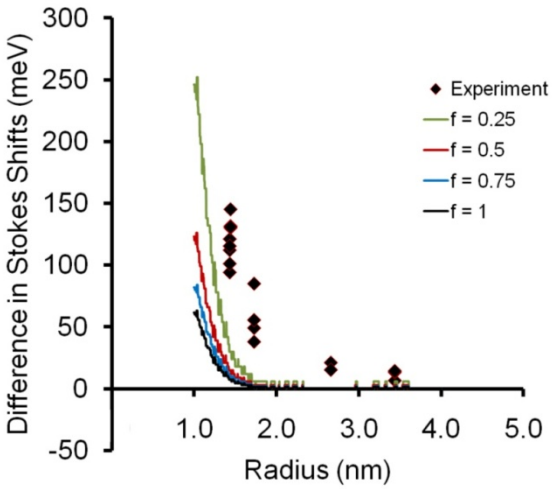

Figure S4. Difference in Stokes shift of NPs and hybrids versus NP radius. Experimental data points are shown, along with solid lines for the phonon model for different values of f (and with $\Delta = 1$ meV and fast energy relaxation, as described in the main paper).

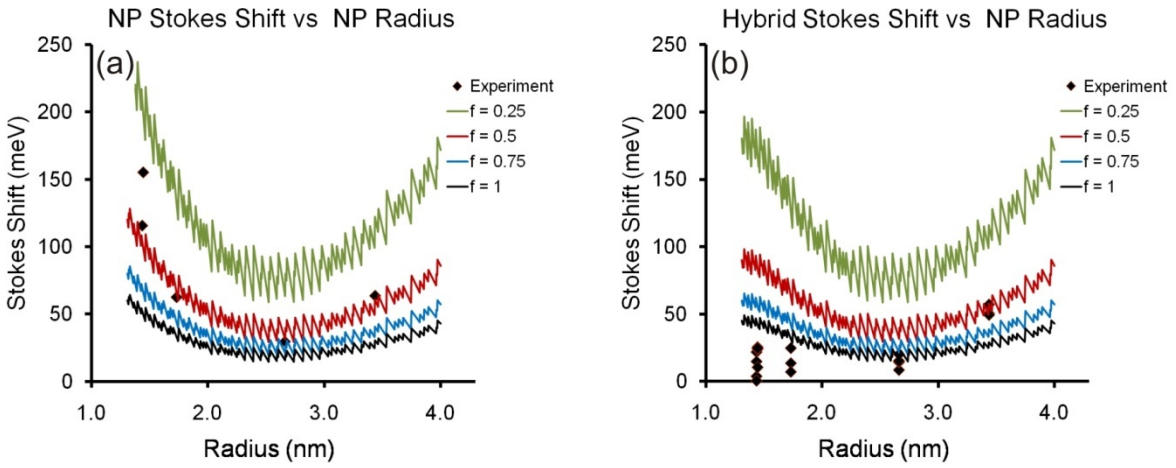

Figure S5. Stokes shift of (a) NPs and (b) hybrids versus NP radius. Experimental data points are shown, along with solid lines for the phonon model for different values of f (and with $\Delta = 1$ meV and fast energy relaxation, as described in the main paper).

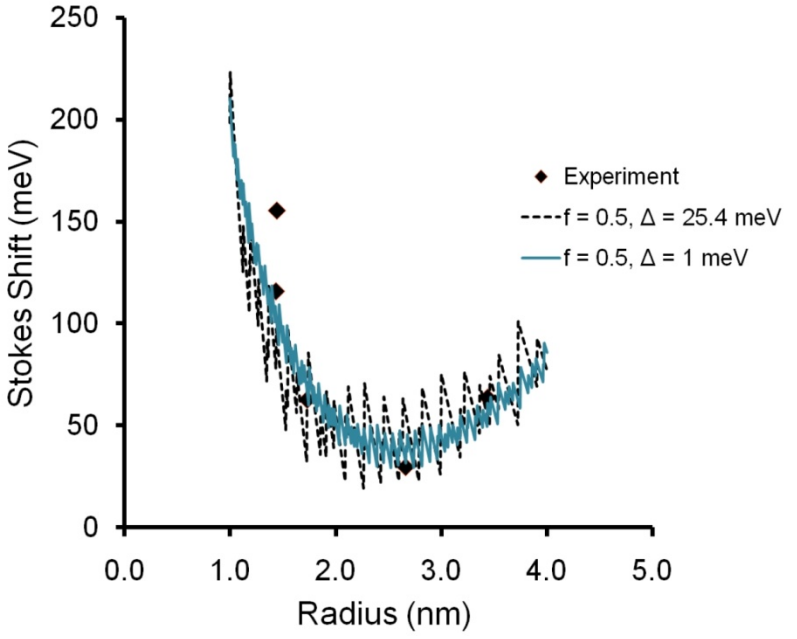

Figure S6. Stokes shift of NPs versus NP radius. Experimental data points are shown, along with solid lines for the phonon model for $\Delta = 1$ meV and 25.4 meV (with $f = 0.5$ and fast energy relaxation, as described in the main paper).

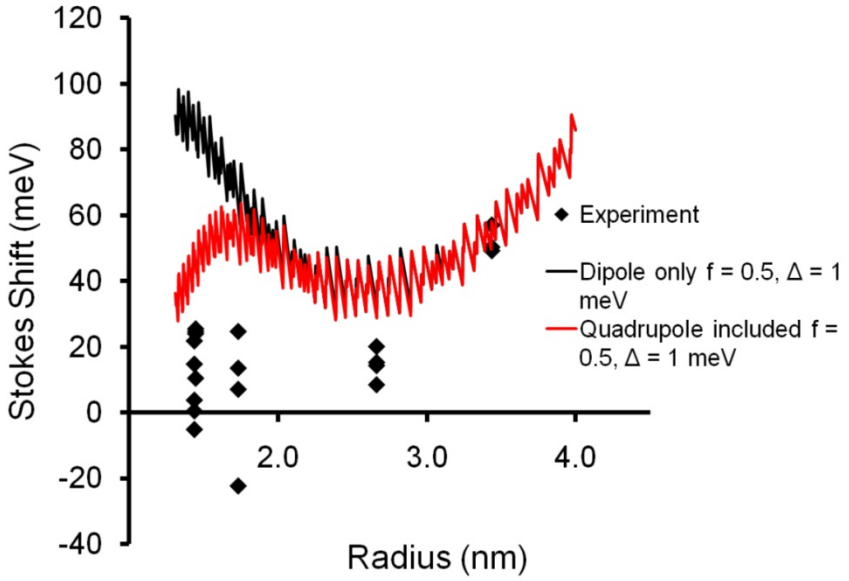

Figure S7. Phonon model predictions of the Stokes shift of the hybrids, including the deviations from dipole-dipole energy transfer, as in Eq. 9.

References:

[1] C. G. Lu, A. Akey, W. Wang, and I. P. Herman, J. Am. Chem. Soc. **131**, 3446 (2009).

[2] J. J. Li, Y. A. Wang, W. Z. Guo, J. C. Keay, T. D. Mishima, M. B. Johnson, and X. G. Peng, J. Am. Chem. S. **125**, 12567 (2003).